Available online at www.sciencedirect.com

ScienceDirect

Procedia Structural Integrity 75 (2025) 426–434

Structural Integrity Procedia

www.elsevier.com/locate/procedia

Fatigue Design 2025 (FatDes 2025)

Enhancing the Lifespan of Steel Structures through a 3D-printed Coating Device for the Application of a Nanometallic Multilayer on Weld Seams

Maren Seidelmann*, Niclas Spalek, Mohsen Falah, Nikolay Lalkovski, Marcus Rutner

Hamburg Institute of Technology, Denickestraße 17, 21073 Hamburg, Germany

Abstract

Given the substantial environmental and economic consequences associated with deteriorating infrastructure, prolonging the service life of steel bridges is essential for advancing sustainability and economic viability. A critical factor in achieving this goal is enhancing the integrity of welded joints, which play a pivotal role in the bridge's performance under dynamic loading conditions. Research indicates that the fatigue strength of welds can be increased by up to sixfold through the application of a nanometallic multilayer (NMM) composed of nickel and copper. To date, investigations into the fatigue enhancement of welded joints using NMM have predominantly been conducted on a laboratory scale. To enable practical application on existing infrastructure, a coating device is being developed to apply the NMM treatment directly onto surfaces without the need for full immersion in an electrolyte bath, thus supporting its implementation as a post-treatment process for steel bridges.

Keywords: Nanometallic Multilayer, Post-weld Treatment, 3D-Printing, In-Situ Coating, Fatigue Resistance, Steel Bridges

1. Introduction

Due to increasing resource scarcity and the ongoing deterioration of the global climate, the conservation of materials and the extension of the service life of steel structures are becoming increasingly important. One of the primary factors contributing to damage and reduced longevity in steel bridges is fatigue failure at welded joints. It is estimated that over 50 % of engineering products worldwide contain weld seams (Aucott et al., 2017). Given that cracks frequently initiate at these locations, the structural integrity of steel structures is critically influenced by the properties of their

10.1016/j.prostr.2025.11.042

welds. The welding process, particularly in the heat-affected zone (HAZ), induces microstructural transformations that can significantly affect the fatigue performance of the component. The thermal input and rapid cooling associated with welding often result in hard and brittle microstructures around the weld seam, potentially compromising the durability of the structure under cyclic loading. Consequently, the development and application of effective post-weld treatment (PWT) techniques aimed at enhancing the fatigue life of welded joints have become a central focus of current research. Nevertheless, conventional PWT methods have not become standard in engineering practice, mainly due to limited reliability or lack of economic efficiency (Kuhlmann et al., 2005; Ummenhofer et al., 2009; Ummenhofer et al., 2005).

To address this, a nanometallic multilayer (NMM) made of copper and nickel is investigated, which is applied via galvanic deposition to welded components and their HAZ to mitigate the negative effects of cyclic loading (Brunow et al., 2022; Brunow & Rutner, 2021; Brunow et al., 2023). During the electrodeposition process, the individual layers introduce residual stresses into the steel surface, which contribute to improving the fatigue properties (Spalek et al., 2025). The NMM also changes the weld seam geometry, reduces surface roughness and protects the coated area from environmental influences.

The NMM has a micrometer thickness and does not lead to stiffness change, compared to other strengthening methods, such as Fiber Metal Laminates (Woelke et al., 2015). The NMM thin film does not contribute in carrying any internal forces. The NMM post-weld treatment has been developed over the last years from small-scale laboratory tests (Brunow et al., 2021; Brunow & Rutner, 2021; Ramezani et al., 2017) to a scalable technology (Brunow et al., 2022) by using electrodeposition, applicable for new and existing structures (Rutner et al., 2024; Rutner et al., 2025) as well as for metal 3D-printed structures (Falah et al., 2025).

Laboratory tests on a small scale have shown the significant potential of the NMM to increase the service life of welded structures under fatigue loading by up to sixfold (Brunow et al., 2023). This paper takes the first step towards the practical application of the NMM on steel bridges. Based on a preliminary finite element analysis using the software COMSOL, a coating device is designed and 3D-printed from PETG (Polyethylene Terephthalate Glycol-modified). This device is used in initial trials to coat butt-welded flat sheets (with a coated area size of 10×10 cm^2). The coating results were validated using residual stress measurements via X-ray diffraction (XRD), and structural characterization using scanning electron microscopy (SEM) and focused ion beam (FIB) cross-sectioning.

2. Application of the NMM

The nanometallic multilayer is applied to the weld seam in a single-bath process by means of galvanic deposition. For this purpose, the sample is completely immersed in an electrolyte bath according to the current state of research, i.e. on a small scale (Brunow et al., 2021; Brunow & Rutner, 2021). The sample, which forms the cathode, and the nickel electrodes, which form the anodes, are connected to an external circuit. By applying a pulse current, nickel or copper (depending on the current intensity) are deposited on the surface of the sample and the nanometallic coating with its layered structure is gradually formed. The current densities used for the deposition of the Cu/Ni nanolaminate are 0.45 mA/cm^2 for Cu deposition and 22 mA/cm^2 for Ni deposition. The electrolyte consists of a citrate Cu/Ni sulphate bath (Bonhôte & Landolt, 1997).

As large built welded structures such as bridges cannot be completely immersed in an electrolyte bath, a way must be found to effectively coat the specific weld seams which are particularly critical in respect to fatigue. The approach developed herein is an in-situ coating device (chapter 3) which is placed on the weld seam for processing the NMM. During this in-situ process, the electrolyte fills the device chamber, hence gets in contact with the steel surface of the bridge in a defined area enabling NMM-coating of this area.

3. Development of the Coating Device

3.1. Definition of the Requirements for the Coating Device

The primary objective is to apply the NMM onto a flat bridge component featuring a double V-weld using the coating device. Applying the nanometallic coating to a real bridge introduces more complex requirements compared to small-scale applications.

These include, but are not limited to, the following considerations:

- **Power Supply:** The power supply to the steel surface to be coated—specifically, the bridge detail—must be ensured in a non-destructive manner. Creating holes for plugs or connection points for terminals is not feasible.
- **Electrolyte Contact and Sealing:** The component to be coated is not fully immersed in the electrolyte solution; instead, it is only in contact with the steel surface in the specified coating area. This necessitates stringent requirements for the sealing of the device. An effective seal must be established between the device and the steel surface, and sufficient contact pressure between the device and the surface must be maintained.
- **Electrolyte Agitation:** Continuous agitation of the electrolyte solution during the coating process is mandatory. While a stirring bar and magnetic stirrer are effective on a small scale, they are inadequate for large-scale applications, requiring alternative solutions.
- **Device Material:** The device is to be fabricated from plastic using 3D printing technology. The low pH value of the electrolyte solution (approximately pH 3-4) necessitates careful material selection to ensure chemical resistance.
- **Positional Coating Requirements:** Coating the weld seams on an actual bridge may require overhead applications, meaning the device must adhere securely to the steel surface without relying on gravity.

All these requirements must be considered in the device design. Special attention must be paid to prevent electrolyte leakage, to ensure adequate power supply to the steel, to maintain independent adhesion of the device to the surface, and to guarantee material resistance to the electrolyte fluid used.

3.2. FE Simulation of the Coating Process

The distance between the steel substrate and the electrode is a key parameter, as it directly affects the deposition rate and resulting layer thickness (Table 1). To identify an optimal spacing, finite element (FE) simulations are performed in COMSOL (Comsol Multiphysics GmbH) for both nickel and copper coatings, systematically varying the electrode-to-surface distance. Target individual layer thicknesses, based on preliminary experiments, are defined as 15 nm for copper and 35 nm for nickel. Simulation results, summarized in Table 1, report coating thicknesses in the middle of the coated steel surface as a function of distance, assuming a fixed electrode area of 10×10 cm^2. For nickel, the layer thickness decreases with increasing distance to the anode, approaching approximately 31 nm asymptotically. Copper follows a similar trend, stabilizing at 16.7–16.8 nm around 45 mm.

Table 1. Individual layer thickness of the Ni- and Cu-layer for different distances between electrode and steel surface (electrode size 10×10 cm^2).

Distance between steel surface and electrode	25 mm	35 mm	40 mm	45 mm	50 mm	55 mm
Layer thickness of Ni-layer	34.85 nm	33.09 nm	32.39 nm	31.83 nm	31.38 nm	31.03 nm
Layer thickness of Cu-layer	17.37 nm	17.1 nm	16.98 nm	16.72 nm	16.79 nm	16.72 nm

The results at a constant distance of 50 mm between the steel surface and the electrode and variation of the electrode surface are shown in Table 2 below. Accordingly, the coating thickness decreases with increasing electrode size. The differences are much more pronounced for the nickel layer than for the copper layer, where the thickness values are in the range of about 17 nm regardless of the electrode size.

Table 2. Individual layer thickness of the Ni- and Cu-layer for different sizes of the electrode (distance between surface and electrode 50 mm).

Size of the electrode	7.5×7.5 cm^2	8×8 cm^2	10×10 cm^2	12×12 cm^2
Layer thickness of Ni-layer	35.7 nm	34.84 nm	31.38 nm	29.51 nm
Layer thickness of Cu-layer	17.34 nm	17.22 nm	16.79 nm	16.47 nm

As illustrated in Figure 1, the coating thickness exhibits significant spatial variation. At the edges, nickel layers reach up to 60 nm (electrode size: 10×10 cm^2; distance: 50 mm), nearly double the thickness at the center (~31 nm). This variation depends strongly on electrode geometry and spacing and cannot be generalized. It is important to note that the pronounced geometric effects observed in the COMSOL simulation may not fully reflect experimental conditions. The model accounts only for secondary current distribution, neglecting factors such as electrolyte

convection and ion concentration gradients. Moreover, the simulation is conducted potentiostatically, while the actual process is galvanostatic. Thus, while certain simulation effects may not occur in practice, the results offer a useful starting point for geometric design considerations.

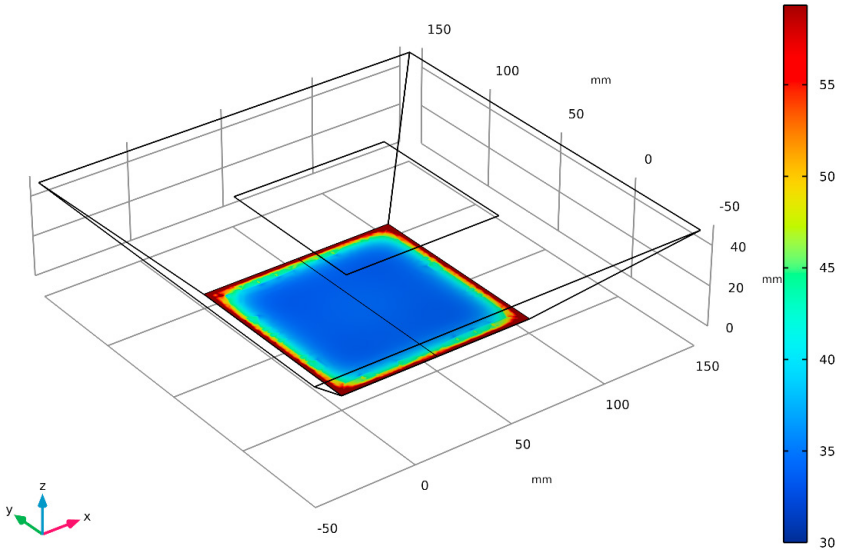

Fig. 1 Total electrode thickness change [nm] for electrode size 10×10 cm^2 and distance between electrode and surface of 50 mm.

Based on the simulation results, an electrode size of 80×80 mm^2 and a distance of 50 mm is selected for the coating device design. These parameters represent a compromise between achieving uniform layer thickness, matching target values from small-scale tests, and ensuring practical implementation. A larger electrode or smaller distance would increase the weight of the device or limit the integration of necessary connections.

4. Design and Manufacturing of the Device

The coating device is designed to meet the requirements outlined in Section 3.1, featuring a modular architecture adaptable to various surface geometries by exchanging individual components. Electrode size and the distance between electrode and steel surface can be adjusted by replacing parts 1 or 2 (Fig. 2). The device comprises four parts: Part 1, which contacts the steel surface and can be tailored to the geometry; Part 2, housing the electrode and its power connection, sealed liquid-tight through the outer wall; Part 3, providing electrolyte volume and securing electrode positioning; and part 4, serving as the lid, equipped with four hose connections for electrolyte supply and removal (Fig. 2). Power to the steel surface is ensured by four spring contacts, modularly attachable to the base to guarantee uniform current distribution. The modules are assembled using side-slidable clips, with flat EPDM (ethylene propylene diene monomer) closed-cell seals applied at joints and contact surfaces to ensure liquid-tight sealing.

The coating device is attached to the steel surface using 8 magnetic feet, which can be switched on and off via a rotary wheel without a power supply. It must be taken into account that the steel surface is magnetized by the magnets. This can affect the galvanic coating (Kołodziejczyk et al., 2018). However, Kołodziejczyk et al. (2018) suggest that this influence can also be positive (reduced grain sizes in the NMM, smoother surface).

The coating device is additively manufactured from PETG. The advantage of using PETG is its increased chemical resistance compared to, for example, PLA (Polylactic Acid) (Algarni & Ghazali, 2021; Valvez et al., 2022). Additionally, PETG is more impact-resistant and stable (Algarni & Ghazali, 2021; Valvez et al., 2022). However, printing PETG is complex and requires specialized 3D printers and carefully selected print settings. The Bambulab X1 Carbon printer is used for manufacturing the coating device.

The coating device has external dimensions of approximately 23×23×25 cm^3 (W×D×H), an inner volume of 2 liters.

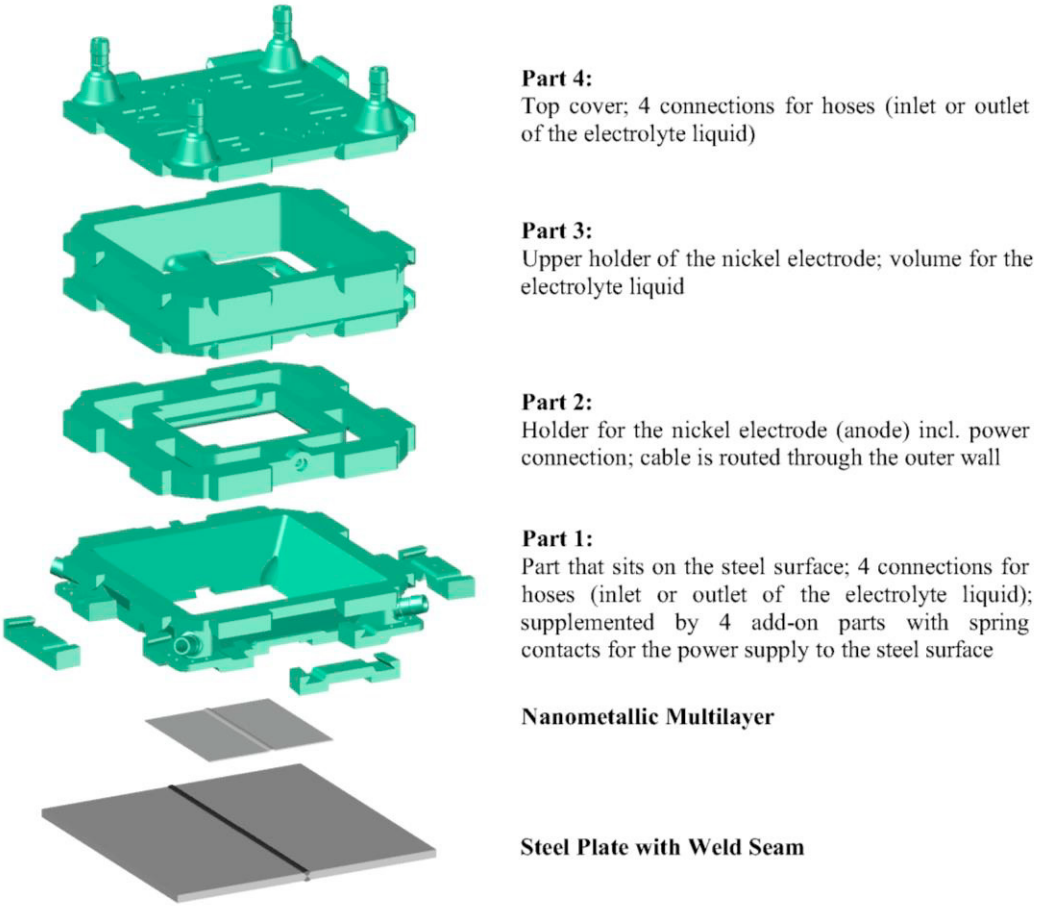

Fig. 2 Composition of the coating device, NMM and steel plate with weld seam.

5. Test Implementation

5.1. Test Specimen

In the initial experiments, a flat, non-welded steel sheet is employed as test specimen. The coating device features four corner holes through which screws are inserted to secure the device directly onto the surface, thereby ensuring adequate contact pressure during the coating process. In further experiments, the container is connected to the surface using magnetic feet, which enables non-destructive coating of the surface. Finally, a sheet with a butt-welded double V-seam is coated locally with the NMM.

5.2. Experimental Setup

The necessary mixing of the electrolyte is achieved by continuously circulating the liquid through the coating device using a peristaltic pump. The electrolyte is supplied via two hoses connected to part 1 of the device, while two hoses connected to part 4 facilitate the discharge.

Each spring contact is equipped with a cable terminating in a plug. These cables are interconnected and connected to the pulse power source. By linking the anode (nickel electrode) to the pulsed current supply, an electrical circuit is established, enabling the galvanic deposition of the coating onto the steel surface. The NMM is deposited using a pulsed current process. Fig. 4 illustrates the successful application of the NMM to a flat sheet featuring a double V-weld, as well as the lower container section equipped with holding magnets.

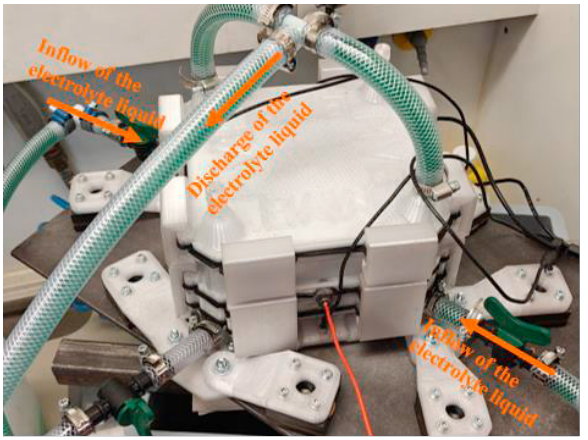

Fig. 3 NMM processing with the in-situ coating device.

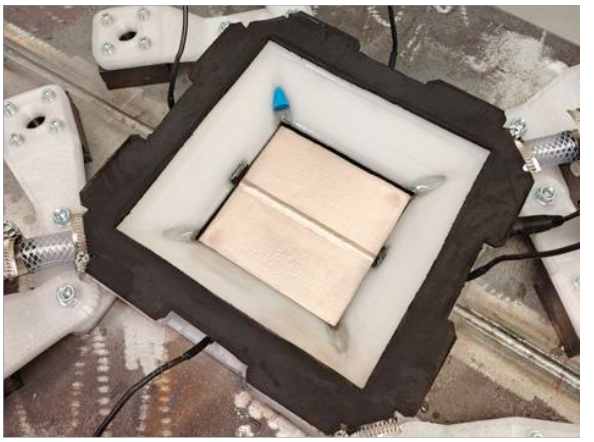

Fig. 4 Successful coating of a butt-welded double V-seam with NMM.

Three additional modular components are attached to each container corner using screws through the four corner holes. Two rigid magnetic feet are mounted at each corner and can be manually activated or deactivated via a rotary switch, independently of external power. Each foot theoretically provides an adhesive force of 65 N, assuming perfect flat contact—though this ideal is not fully achieved due to the limited compressibility of the sealing layer between the container and steel surface. Nevertheless, the eight symmetrically arranged magnetic feet provide sufficient contact pressure for stable operation.

6. Results

6.1. Surface of the NMM

The tests on the flat sheets without weld seam showed a significant influence of the pump speed on the coating result. The aim is to achieve a uniform, slightly shiny silver coating without dark discolored areas. Fig. 5 left shows that pumping in the electrolyte liquid too strongly, leads to strong discoloration of the NMM in the upper left and lower right corners. Reducing the pumping speed to approx. 50 % of the value in Fig. 5 left led to a better result, see Fig. 5, right image.

Fig. 5 Coating of flat sheets; from left to right reduction of the pump speed of the peristaltic pump (left: 5.9 l/min; middle: 4.4 l/min; right: 2.8 l/min).

Fig. 6 presents the surface morphology of the NMM at an approximate distance of 3 cm from the outer edge of the patch under SEM (scanning electron microscopy). The surface appears smooth and homogeneous.

Fig. 7 shows the edge of the NMM coating. The left half of the figure shows the uncoated steel surface, while the right half shows the significantly smoother surface of the NMM. In the edge area, the NMM is jagged and apparently does not adhere perfectly to the surface everywhere. Holes can also be seen in the coating. It is therefore advisable to slightly overlap the deposited patches of the NMM (e.g. 1 cm) in order to prevent defects in the edge areas leading to a limited function of the NMM.

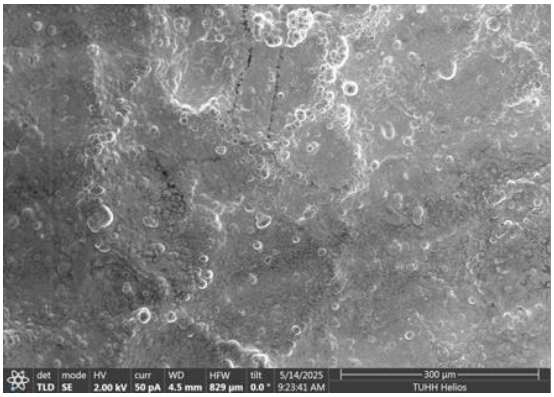

Fig. 6 Surface of the NMM under SEM.

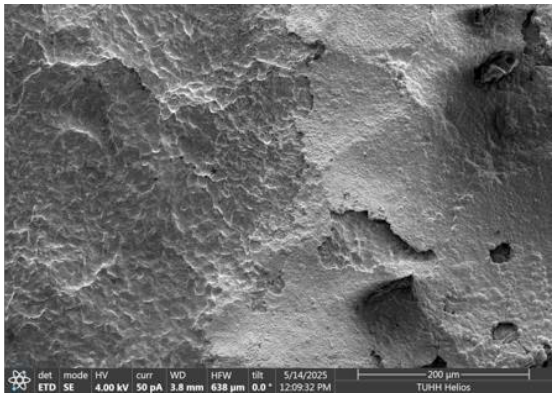

Fig. 7 Edge area of the NMM (transition to steel) under SEM.

6.2. Examination of the Layer Structure via FIB Cross-Sectioning

The layer structure of the coating process is observed using FIB Cross-Sectioning. For better recognizability under the microscope, the coating thicknesses are selected as 10 nm (copper) and 100 nm (nickel) instead of 15 nm and 35 nm, as was previously the case on a small scale. The laminar structure of the coating is clearly recognizable in Fig. 8. The steel section is visible in dark gray at the lower end of Fig. 8. While the desired total layer thickness is 9240 nm, the measured total layer thickness of 9500 nm is achieved (approx. 2.8 % increase).

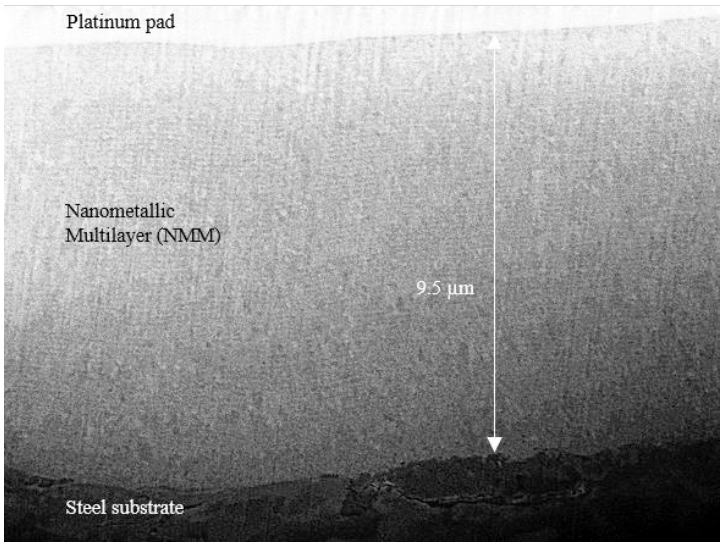

Fig. 8 Layer structure of the NMM processed by the coating device (FIB).

6.3. Examination of the Residual Stresses via XRD

To characterize residual stresses potentially introduced by the application of the NMM, X-ray diffraction measurements are conducted using the Xstress DR45 system (Stresstech®, Ireland), equipped with 2D detectors offering a spatial resolution of 256×256 pixels and a pixel size of 55 µm. Data analysis employed polynomial regression according to the Savitzky-Golay algorithm (Savitzky & Golay, 1964). Measurements targeted the crystallographic {220} planes of Ni and Cu, utilizing Cr Kα radiation ($\lambda = 0.229107$ nm). The ψ-tilt range spanned –45.0° to +45.0°, with an exposure time of 5 seconds per frame. Diffraction patterns are centered at mean 2θ angles of 127.4° and 133.7°, yielding critical information on lattice strain and parameter variations.

The substrate surface is prepared by steel blast cleaning prior to NMM application, inducing compressive residual stresses, consistent with expectations by Totten (2002). For the Fe {211} reflection, a compressive stress magnitude of 275 MPa is recorded. In NMM-coated areas, stress analysis is confined to the Ni and Cu layers due to the limited X-ray penetration depth, precluding direct assessment of the steel substrate. Residual stress measurements are conducted on Ni {220} ($2\theta = 133.7°$) and Cu {220} ($2\theta = 127.4°$), revealing tensile stresses of 650 MPa in nickel and 350 MPa in copper. The NMM architecture consisted of alternating 10/100 nm layers, as confirmed by FIB analysis. The tensile nature of the measured stresses suggests a balancing compressive field within the substrate. It is anticipated that altering the NMM layer periodicity (e.g., to 15/35 nm or 5/35 nm) could further tailor the stress state.

Residual stress measurements in the corner regions of the NMM, where the electrolyte is pumped into the system, revealed notably lower values—approximately 340 MPa in Ni and 200 MPa in Cu—compared to other areas. SEM analysis suggests that this reduction is due to suboptimal adhesion and compromised NMM quality in these zones. Given that the NMM layer extends significantly beyond the HAZ of the weld seam, the localized degradation is not deemed detrimental to the overall performance of the NMM.

7. Conclusion and Outlook

Using the presented coating device, it has been successfully demonstrated that nanometallic multilayers (NMM) composed of nickel and copper can be deposited onto a steel surface without immersing the entire component in the electrolyte solution. The achieved layer thicknesses closely correspond to the expected values, with a deviation of only 2.8 % in total layer thickness.

Furthermore, X-ray diffraction analysis (XRD) confirmed the occurrence of residual tensile stresses in the NMM, resulting in residual compressive stresses in the steel surface in the coated area. According to current research, these residual stresses are the most significant mechanism by which the NMM extends the service life of welded steel structures. Thus, the developed coating device represents a crucial first step toward applying nanolaminates as a post-weld treatment method for existing bridge structures.

Future studies should investigate whether the magnetic field generated by the fastening magnets significantly influences the electroplating process and, if so, whether this effect is beneficial or detrimental. Additionally, the modular coating container is being further developed to allow operation in an inverted position (rotated by 180°). This overhead applicability is essential for the application of NMM coatings on existing bridge structures.

Moreover, investigations into the effect of localized NMM coatings on the corrosion behavior of existing bridge structures should be conducted, since nickel and especially copper are more noble than structural steel.

References

Algarni, M., & Ghazali, S. (2021). Comparative Study of the Sensitivity of PLA, ABS, PEEK, and PETG's Mechanical Properties to FDM Printing Process Parameters. *Crystals*, *11*(8), 995. https://doi.org/10.3390/cryst11080995

Aucott, L., Huang, D., Dong, H. B., Wen, S. W., Marsden, J. A., Rack, A., & Cocks, A. C. F. (2017). Initiation and growth kinetics of solidification cracking during welding of steel. *Scientific Reports*, *7*, 40255. https://doi.org/10.1038/srep40255

Bonhôte, C., & Landolt, D. (1997). Microstructure of Ni-Cu multilayers electrodeposited from a citrate electrolyte. *Electrochimica Acta*, *42*(15), 2407–2417. https://doi.org/10.1016/S0013-4686(97)82474-7

Brunow, J., Gries, S., Krekeler, T., & Rutner, M. (2022). Material mechanisms of Cu/Ni nanolaminate coatings resulting in lifetime extensions of welded joints. *Scripta Materialia*, *212*, 114501. https://doi.org/10.1016/j.scriptamat.2022.114501

Brunow, J., Ritter, M., Krekeler, T., Ramezani, M., & Rutner, M. (2021). Thermal stability of a nanolayered metal joint. *Scripta Materialia*, *194*, 113687. https://doi.org/10.1016/j.scriptamat.2020.113687

Brunow, J., & Rutner, M. (2021). Das Nanolaminatpflaster – Schweißnahtnachbehandlung für bisher unerreichte Lebensdauerverlängerung. *Stahlbau*, *90*(9), 691–700. https://doi.org/10.1002/stab.202100042

Brunow, J., Spalek, N., Mohammadi, F., & Rutner, M. (2023). A novel post-weld treatment using nanostructured metallic multilayer for superior fatigue strength. *Scientific Reports*, *13*(1), 22215. https://doi.org/10.1038/s41598-023-49192-0

Falah, M., Spalek, N., Seidelmann, M., Lalkovski, N., & Rutner, M. (2025). Significant improvement of the fatigue performance of ER70S-6 WAAM un-milled structures: A Cu/Ni multilayer nanotechnology approach. *Structural Integrity Procedia*.

Kołodziejczyk, K., Miękoś, E., Zieliński, M., Jaksender, M., Szczukocki, D., Czarny, K., & Krawczyk, B. (2018). Influence of constant magnetic field on electrodeposition of metals, alloys, conductive polymers, and organic reactions. *Journal of Solid State Electrochemistry*, *22*(6), 1629–1647. https://doi.org/10.1007/s10008-017-3875-x

Kuhlmann, U., Bergmann, J., Dürr, A., Thumser, R., Günther, H.-P., & Gerth, U. (2005). Erhöhung der Ermüdungsfestigkeit von geschweißten höherfesten Baustählen durch Anwendung von Nachbehandlungsverfahren. *Stahlbau*, *74*(5), 358–365. https://doi.org/10.1002/stab.200590066

Ramezani, M. G., Demkowicz, M. J., Feng, G., & Rutner, M. P. (2017). Joining of physical vapor-deposited metal nano-layered composites. *Scripta Materialia*, *139*, 114–118. https://doi.org/10.1016/j.scriptamat.2017.06.032

Rutner, M., Lalkovski, N., Falah, M., Seidelmann, M., & Spalek, N. (2025). Merging nano and macro structure design: Opportunities for the structural integrity of steel infrastructure. *Structural Integrity Procedia*.

Rutner, M., Spalek, N., Falah, M., & Lalkovski, N. (2024). Verknüpfung von Nano mit Makro – Chancen für den Stahlbau. *Stahlbau*, *93*(9), 584–596. https://doi.org/10.1002/stab.202400048

Savitzky, A., & Golay, M. J. E. (1964). Smoothing and Differentiation of Data by Simplified Least Squares Procedures. *Analytical Chemistry*, *36*(8), 1627–1639. https://doi.org/10.1021/ac60214a047

Spalek, N., Falah, M., Seidelmann, M., Lalkovski, N., Abreu Faria, G., & Rutner, M. (2025). Material mechanisms of the nanostructured metallic multilayer post-weld treatment for fatigue strength increase. *Structural Integrity Procedia*.

Totten, G. E. (2002). *Handbook of Residual Stress and Deformation of Steel*. A S M International. https://ebookcentral.proquest.com/lib/kxp/detail.action?docID=3002377

Ummenhofer, T., Herion, S., & Weich, I. (2009). Schweißnahtnachbehandlung mit höherfrequenten Hämmerverfahren – Ermüdungsfestigkeit, Qualitätssicherung, Bemessung. *Stahlbau*, *78*(9), 605–612. https://doi.org/10.1002/stab.200910074

Ummenhofer, T., Weich, I., & Nitschke-Pagel, T. (2005). Lebens- und Restlebensdauerverlängerung geschweißter Windenergieanlagentürme und anderer Stahlkonstruktionen durch Schweißnahtnachbehandlung. *Stahlbau*, *74*(6), 412–422. https://doi.org/10.1002/stab.200590085

Valvez, S., Silva, A. P., & Reis, P. N. B. (2022). Optimization of Printing Parameters to Maximize the Mechanical Properties of 3D-Printed PETG-Based Parts. *Polymers*, *14*(13). https://doi.org/10.3390/polym14132564

Woelke, P. B., Rutner, M. P., Shields, M. D., Rans, C., & Alderliesten, R. (2015). Finite Element Modeling of Fatigue in Fiber–Metal Laminates. *AIAA Journal*, *53*(8), 2228–2236. https://doi.org/10.2514/1.J053600